







ORIGINAL ARTICLE

Brain glucose uptake is associated with endogenous glucose production in obese patients before and after bariatric surgery and predicts metabolic outcome at follow-up

Eleni Rebelos¹  | Heidi Immonen¹ | Marco Bucci¹  | Jarna C. Hannukainen¹  |
Lauri Nummenmaa^{1,2} | Miikka-Juhani Honka¹  | Minna Soinio³ | Paulina Salminen⁴ |
Ele Ferrannini⁵  | Patricia Iozzo^{1,5} | Pirjo Nuutila^{1,3} 

¹Turku PET Centre, University of Turku, Turku, Finland

²Department of Psychology, University of Turku, Turku, Finland

³Department of Endocrinology, Turku University Hospital, Turku, Finland

⁴Department of Digestive Surgery and Urology, Turku University Hospital, Turku, Finland

⁵Institute of Clinical Physiology, National Research Council (CNR), Pisa, Italy

Correspondence

Pirjo Nuutila, Turku PET Centre, Department of Endocrinology and University of Turku, Turku University Hospital, Turku, Finland.
Email: pirjo.nuutila@utu.fi

Funding information

The study was conducted within the Center of Excellence in Cardiovascular and Metabolic Diseases, supported by the Academy of Finland, the University of Turku, Turku University Hospital, and Åbo Akademi University. Additional funding was received from the Finnish Diabetes Foundation, the Sigrid Juselius Foundation, the Academy of Finland (grants 256 147 and 251 125 to L.N.), and an Aivo-Aalto grant of Aalto University.

Aims: To investigate further the finding that insulin enhances brain glucose uptake (BGU) in obese but not in lean people by combining BGU with measures of endogenous glucose production (EGP), and to explore the associations between insulin-stimulated BGU and peripheral markers, such as metabolites and inflammatory markers.

Materials and methods: A total of 20 morbidly obese individuals and 12 lean controls were recruited from the larger randomized controlled SLEEVEPASS study. All participants were studied under fasting and euglycaemic hyperinsulinaemic conditions using fluorodeoxyglucose-positron emission tomography. Obese participants were re-evaluated 6 months after bariatric surgery and were followed-up for ~3 years.

Results: In obese participants, we found a positive association between BGU and EGP during insulin stimulation. Across all participants, insulin-stimulated BGU was associated positively with systemic inflammatory markers and plasma levels of leucine and phenylalanine. Six months after bariatric surgery, the obese participants had achieved significant weight loss. Although insulin-stimulated BGU was decreased postoperatively, the association between BGU and EGP during insulin stimulation persisted. Moreover, high insulin-stimulated BGU at baseline predicted smaller improvement in fasting plasma glucose at 2 and 3 years of follow-up.

Conclusions: Our findings suggest the presence of a brain-liver axis in morbidly obese individuals, which persists postoperatively. This axis might contribute to further deterioration of glucose homeostasis.

KEYWORDS

bariatric surgery, brain glucose uptake, endogenous glucose production, insulin resistance, obesity, positron emission tomography

1 | INTRODUCTION

Brain glucose metabolism has long been considered not to be influenced by insulin, but this view has recently been challenged.^{1,2} Insulin receptors are found throughout the human brain, with especially high concentrations in the hypothalamus, cerebellum and cortex.³

Although the peripheral effects of insulin are well known, the central effects of insulin on the human brain remain poorly understood.

Moreover, whether insulin action in the brain can affect peripheral glucose metabolism, namely, glucose production and utilization, has not been extensively assessed in humans. A connection between brain and endogenous glucose production (EGP) is of special interest as deregulation of insulin-induced EGP suppression is a characteristic of type 2 diabetes (T2D) that contributes to fasting hyperglycaemia.⁴

In an early animal study, activation of the ventromedial nucleus of the hypothalamus was found to increase plasma glucose levels by

accelerating glycogenolysis in the liver, suggesting that the hypothalamus could directly control EGP.⁵ Later work in rats showed that administration of insulin agonists directly into the third cerebral ventricle suppresses EGP.⁶ This effect was thought to operate through the phosphatidylinositol-3-kinase pathway as it was abolished by administration of K_{ATP} inhibitors.⁶ Moreover, insulin in the brain activates the hepatic signal transducer and activator of transcription 3 (STAT3) in a process involving interleukin-6 (IL-6), as demonstrated by the fact that disturbing IL-6 signalling abolished insulin-induced phosphorylation of hepatic STAT3 and attenuated EGP suppression.⁷ Several lines of research have provided evidence that central glucose sensing, involving glucose-regulated neurons as well as astrocytes, may also modulate EGP.⁸

Recent findings on brain insulin action in larger animals and humans support the existence of a "brain-liver axis". Although insulin administration into the head arteries of dogs did not suppress hepatic glucose production, hepatic glycogen synthesis was increased and mRNA expression of gluconeogenic enzymes was decreased.⁹ In a small study in humans, Dash et al.¹⁰ showed that intranasal insulin administration suppresses EGP during a pancreatic clamp. In addition, Heni et al.¹¹ have recently demonstrated that intranasal insulin application decreases EGP in lean but not in overweight subjects.

We previously showed that insulin stimulation enhances brain glucose uptake (BGU), measured with fluorodeoxyglucose (^{18}F -FDG) positron emission tomography (PET), as compared to fasting, in obese individuals and in individuals with impaired glucose tolerance but not in lean individuals or those with normal glucose tolerance.^{12,13} The molecular mechanism of this phenomenon is thus far unknown. Moreover, suppression of EGP during hyperinsulinaemic conditions is impaired in obese as compared to lean individuals¹⁴; therefore, we hypothesized that the two variables (ie, BGU and EGP) might be interrelated in morbidly obese individuals. The aim of the present study was to test whether BGU was associated with EGP in humans. Moreover, possible associations between insulin-stimulated BGU and peripheral markers such as metabolites and inflammatory markers were also explored.

2 | MATERIALS AND METHODS

2.1 | Study population

This study follows up on a previous study, the rationale and methodology of which have been published.^{13,15,16} In brief, 20 morbidly obese individuals were recruited as part of a larger randomized, controlled clinical study comparing laparoscopic sleeve gastrectomy ($n = 9$) with Roux-en-Y gastric bypass (RYGB, $n = 11$) in the treatment of morbid obesity (the SLEEVEPASS study, NCT00793143).¹⁶ Individuals with T2D used only metformin (1-3 g daily); those on insulin treatment were excluded from the study. Other inclusion criteria have been previously described.¹⁶ Twelve healthy, lean control individuals were recruited via an advertisement in local newspapers.

2.2 | Study design

All participants underwent a screening visit before inclusion in the study. At the visit, an oral glucose tolerance test (OGTT) was

performed, with blood samples drawn before and at 30, 60, 90 and 120 minutes for glucose, insulin and C-peptide measurements. Fasting blood samples for metabolomics were also collected. At baseline, magnetic resonance imaging (MRI) and two ^{18}F -FDG PET studies, the first in the fasting state and the second during euglycaemic hyperinsulinaemia, were performed and both these measurements were repeated 6 months after bariatric surgery.¹⁷ The PET studies were performed on separate days, <2 weeks apart. Baseline studies were carried out before the obese participants started a 4-week very-low-energy dietary regime prior to the surgery. A total of 17 participants completed the studies after surgery, because three did not return for the post-surgery studies for personal reasons. In one participant, steady-state was not achieved during the euglycaemic clamp and her study was therefore excluded from the analysis (laparoscopic sleeve gastrectomy, $n = 8$; RYGB, $n = 8$). Healthy participants were studied once. MRI was performed after 2 to 3 hours of fasting, and PET studies after an overnight fast. Strenuous physical activity was prohibited from the preceding evening. Anti-diabetic treatment was withheld 24 to 72 hours before the metabolic studies. Obese participants were followed for up to 3 years after bariatric surgery. At the follow-up visits, body weight, body mass index (BMI), fasting plasma glucose, and glycated haemoglobin (HbA_{1c}) were recorded. Prior to inclusion, each participant provided written consent. The study protocol was approved by the Ethics Committee of the Hospital District of Southwest Finland and conducted in accordance with the Declaration of Helsinki.

2.3 | PET study protocol and data acquisition

The studies were performed after a 12-hour fast using the GE Advance PET camera (General Electric Medical Systems, Milwaukee, Wisconsin). The euglycaemic hyperinsulinaemic clamp technique was applied as previously described.¹⁸ In brief, in all 20 obese and 12 lean participants a primed-continuous insulin infusion (at a rate of 40 mU/ m^2 /min) was started and continued until the end of the study (Actrapid; Novo Nordisk, Copenhagen, Denmark). During the clamp, a variable rate of a 20% glucose solution was infused to maintain plasma glucose concentration at 5 mmol/L. Plasma glucose levels were measured every 5 to 10 minutes throughout the clamp. At 100 ± 10 minutes into the clamp, ^{18}F -FDG (187 ± 9 MBq) was injected intravenously over 15 seconds, and radioactivity in the brain was followed thereafter for 40 minutes (4×30 -, 3×60 - and 7×300 -second frames). The PET study protocols are described in more detail in previous reports^{13,17} (Figure S1A). ^{18}F -FDG was synthesized using computer-controlled apparatus.¹⁹ All data were corrected for dead time, decay and measured photon attenuation, and reconstructed using a Hann filter with a cut-off frequency of 0.5 and a median root prior reconstruction method.²⁰ Arterialized blood samples were drawn during the scan and analysed for radioactivity concentration in plasma using an automatic γ counter (Wizard 1480; Wallac, Turku, Finland). During the clamp, plasma glucose, serum insulin and free fatty acids were taken at baseline and every 5, 30 and 60 minutes, respectively.

2.4 | Quantification of brain glucose metabolism

The influx constant (K_i) was calculated for each voxel separately using the linear Gjedde-Patlak plot with the arterial plasma input function, with a linear phase start time of 20 minutes. BGU ($\mu\text{mol}/100 \text{ g}/\text{min}$) was then calculated at voxel level as follows: $BGU_{\text{glu}} = K_i C_p / LC$, where C_p is the average plasma glucose concentration from the injection until the end of the brain scan, and LC is the lumped constant for the brain (which was set at 0.65).²¹ Brain density was set at 1.04.²² Summed PET images were spatially normalized to the ^{18}F -FDG template in Montreal Neurological Institute space (MNI International Consortium for Brain Mapping) using statistical parametric mapping (SPM [SPM12; www.fil.ion.ucl.ac.uk/spm/]) running on Matlab for windows (version 9.1.0; Math Works, Natick, Massachusetts). Normalization variables were subsequently applied to corresponding parametric glucose metabolism images. Parametric images were smoothed at 10 mm full-width at half-maximum. Eight brain regions of interest (ROIs; anterior cerebellum, posterior cerebellum, frontal lobe, limbic lobe, mid-brain, occipital lobe, parietal lobe, temporal lobe) were selected via *wfu pickatlas* (www.fmri.wfubmc.edu/cms/software) and extracted from the BGU parametric images via Marsbar (<http://marsbar.sourceforge.net>) in order to perform the heat map analysis and linear regressions with EGP.

2.5 | Calculations

The EGP values and insulin-stimulated glucose disposal (M -values) were calculated as previously described.^{15,23} Briefly, EGP during the euglycaemic hyperinsulinaemic clamp is calculated by subtracting the exogenous glucose infusion rate from the rate of disappearance of glucose ($EGP = R_d + V_{\text{glucose}} \times \Delta_{\text{glucose}} / \Delta_T$ - glucose infusion rate), where R_d is the rate of disappearance, V_{glucose} is the estimated glucose distribution volume (0.19 L/kg), Δ_{glucose} is the change in glucose from ^{18}F -FDG injection to the end of sampling (mmol/L), and Δ_T is the time of ^{18}F -FDG injection to the end of sampling (minutes). R_d is calculated from the following equation: $R_d = (\text{dose}_{\text{FDG}} - \text{urine}_{\text{FDG}}) / \text{AUC}_{\text{FDG}} \times \text{avg}_{\text{glucose}}$, where $\text{avg}_{\text{glucose}}$ is the average glycaemia from the time of FDG injection to the end of sampling, AUC_{FDG} is the area under the curve of ^{18}F -FDG in plasma from ^{18}F -FDG injection to the end of sampling, and $\text{urine}_{\text{FDG}}$ is the decay-corrected quantity of ^{18}F -FDG measured in the total volume of urine from ^{18}F -FDG injection to the end of the PET scan. In the fasting state, EGP is equal to R_d . Insulin clearance was calculated from the OGTT as mean insulin secretion divided by mean insulin concentration.²⁴

2.6 | Statistical analysis

Data are presented as mean \pm SD (or median [interquartile range] for non-normally distributed variables). Linear regressions were performed in SPM to evaluate correlations between BGU and single regressors (EGP, inflammatory markers, metabolites, follow-up variables) while controlling for confounding factors (setting 0 in the contrasts). Scatterplots of the associations are presented next to each SPM image to aid visualization of the results. To determine these scatterplots, we extracted either (1) mean BGU values from whole-brain ROIs for global effects, or (2) mean BGU values from only the voxels that were identified as being significant in SPM analyses, in which the

effect was not global (presented as BGU^* , as in Figure 2A and Figure S2A). These values were then regressed against the different variables (EGP, inflammatory markers, metabolites, follow-up variables). The results, visualized in scatterplot data, were used to support interpretation of the corresponding SPM analyses; all statistical inference was however based on the whole-brain SPM analyses. Comparisons between groups and time (before vs after surgery) were performed in SPM analysis with a two-sample independent (for groups) or paired (for intervention) t tests. The statistical threshold in SPM analysis was set at a cluster level and corrected with false discovery rate (FDR) with $P < 0.05$. Further statistical analyses were performed using JMP version 13.0 (SAS Institute, Cary, North Carolina). Linear regression between BGU and EGP was also performed for each of the eight ROIs. Comparisons between groups were performed using the t test for normally distributed variables and the Mann-Whitney U test for non-normally distributed variables; paired t tests or Wilcoxon signed rank test for non-parametric variables were performed to assess if there was any difference within participants between preoperative and postoperative data. Associations between circulating metabolites and insulin-stimulated BGU were tested using Spearman ρ correlation coefficient. Heat maps were created using R 3.1.0 package *gplots*.^{25,26} A P value ≤ 0.05 was considered statistically significant. Control for FDR in multiple testing was done using the Benjamini-Hochberg procedure.²⁷ FDR was set at 5%. Post hoc power calculation analysis based on the BGU of the two groups (obese and lean), with significance level set $\alpha = 0.05$, yielded a power ($1-\beta$) of 0.96. Post hoc power calculation analysis on a linear bivariate regression (for BGU and EGP) with significance level set $\alpha = 0.05$ yielded a power ($1-\beta$) of 0.93 in the whole dataset, 0.87 in the obese participants and 1 in the lean participants (*G*Power* 3.1).

3 | RESULTS

3.1 | Before surgery

Obese participants had higher glucose and lipid profiles, and higher hepatic enzymes as compared with lean controls. IL-6, high-sensitivity C-reactive protein (hsCRP) and leptin levels were higher in the obese participants as compared to the age-matched lean controls (Table 1).

In the overnight fasted state, BGU was not different between obese and lean participants.¹³ EGP was higher in the obese as compared with the lean participants when expressed in $\mu\text{mol}/\text{min}$ (Table 1). During the clamp, plasma glucose levels were stable and similar between obese participants and controls throughout the study (Figure S1B). Although the exogenous insulin infusion was adjusted for body surface area, steady-state plasma insulin levels were higher in obese participants as a result of lower insulin clearance (Figure S1C and Table 1). As expected, obese participants had lower M -values and higher insulin-suppressed EGP, the two variables being reciprocally related in the whole dataset (Figures S1D-F). Insulin-stimulated BGU was $\sim 10\%$ higher in obese as compared to control participants (Figure 1A,D).¹³ Different plasma insulin levels between groups did not account for the difference in BGU . In the whole dataset, insulin-stimulated BGU and insulin-suppressed EGP were positively

TABLE 1 Comparisons between obese and lean participants before and after surgery

	Controls	Obese participants: pre-surgery	Obese participants: post-surgery	P ¹	P ²	P ³
n	12	20	16	-	-	-
Men/women	4/8	1/19	0/16	-	-	-
NGT/IGT/T2D	9/3/0	4/10/6	13/2/1	<0.0001	0.0009	0.4
Age, y	43 ± 11	46 ± 9	47 ± 9	0.4	-	0.6
Body weight, kg	68.1 [8.1]	118.4 [17.9]	87.5 [18.5]	<0.0001	<0.0001	<0.0001
BMI, kg/m ²	23.2 [3.0]	43.1 [2.5]	32.2 [3.1]	<0.0001	<0.0001	<0.0001
Fat mass, %	32.4 [9.1]	48.1 [1.7]	41.9 [3.0]	<0.0001	<0.0001	<0.0001
Fasting plasma glucose, mmol/L	5.5 ± 0.4	6.2 ± 0.8	5.4 ± 0.5	0.01	0.0002	0.4
Insulin clearance, L/min/m ²	1.5 ± 0.3	1.1 ± 0.3	1.3 ± 0.3	0.004	0.0002	0.08
HbA1c				0.08	0.04	0.7
mmol/mol	37 ± 3.4	40 ± 5.1	37 ± 3.6			
%	5.6 ± 0.3	5.8 ± 0.5	5.5 ± 0.3			
Leptin, ng/mL	15.5 [14]	55.7 [23]	26.9 [15]	0.0002	<0.0001	0.01
IL-6, pg/mL	1.1 [1.2]	2.6 [2.0]	1.9 [0.6]	0.02	0.02	0.1
hsCRP, mg/L	0.8 [1.3]	3.2 [5.1]	1.0 [1.8]	0.003	0.009	0.3
Total cholesterol, mmol/L	5.1 ± 0.8	4.4 ± 0.8	4.2 ± 0.5	0.04	0.4	0.004
HDL cholesterol, mmol/L	1.9 ± 0.5	1.3 ± 0.2	1.5 ± 0.2	0.003	0.01	0.02
LDL cholesterol, mmol/L	3.0 ± 0.7	2.8 ± 0.7	2.5 ± 0.5	0.5	0.3	0.07
Triglycerides, mmol/L	0.9 ± 0.4	1.3 ± 0.4	0.9 ± 0.2	0.006	0.005	0.4
ALT, U/L	17 ± 7	31 ± 12	19 ± 10	0.0007	0.01	0.7
AFOS, U/L	47 ± 10	64 ± 22	62 ± 20	0.05	0.5	0.07
gGT, U/L	15 [13]	30 [18]	13 [8]	0.0006	0.2	0.4
Steady-state insulin, pmol/L	392 ± 94	518 ± 190	467 ± 76	0.04	0.3	0.03
Steady-state glucose, mmol/L	5.1 [0.2]	5.0 [0.1]	5.2 [0.1]	0.4	0.2	0.8
Coefficient of variation, %	7.6	7.4	9.2			
M-value, µmol/kgFFM/min	67.3 [43.3]	25.2 [23.0]	52.1 [34.0]	<0.0001	<0.0001	0.05
Fasting EGP, µmol/kgFFM/min	15.49 [2.78]	14.82 [4.68]	14.76 [3.25]	0.8	0.5	0.2
Fasting EGP, µmol/min	724 [142]	899 [311]	754 [236]	0.0004	<0.0001	0.7
EGP clamp, µmol/kgFFM/min	0.27 [7.74]	6.20 [8.18]	3.6 [5.56]	0.03	0.8	0.06
EGP clamp, µmol/min	12 [351]	390 [522]	208 [318]	0.006	0.9	0.5
% suppression as compared to fasting	99	54	74			

Abbreviations: AFOS, alkaline phosphatase; ALT, alanine transaminase; BMI, body mass index; EGP, endogenous glucose production; FFM, fat free mass; gGT, gamma-glutamyltransferase; HbA1c, glycated haemoglobin; hsCRP, high-sensitivity C-reactive protein; IGT, impaired glucose tolerance; IL, interleukin; NGT, normal glucose tolerance; T2D, type 2 diabetes.

Values are mean ± SD or median [interquartile range]. P¹ = P value for the comparison of obese patients pre-surgery versus lean controls; P² = P value for the comparison of obese patients pre- versus post-surgery; P³ = P value for the comparison of obese patients post-surgery versus lean controls.

associated ($r = 0.51$, $P = 0.003$), although the association was driven by the obese group ($r = 0.60$, $P = 0.006$ in obese participants; $r = -0.1$, $P = 0.7$ in lean participants [Figure 1B,C,E,F]). The association between insulin-stimulated BGU and insulin-suppressed EGP remained significant after accounting for BMI ($r = 0.66$, $P = 0.009$) or steady-state insulin ($r = 0.54$, $P = 0.003$).

Similarly, at the level of the ROIs that were specifically examined, in the obese participants the positive association between BGU and EGP was detected across all of them (anterior cerebellum: $r = 0.59$, $P = 0.007$; posterior cerebellum: $r = 0.52$, $P = 0.02$; frontal lobe: $r = 0.64$, $P = 0.003$; limbic lobe: $r = 0.63$, $P = 0.003$; midbrain: $r = 0.57$, $P = 0.009$; occipital lobe: $r = 0.59$, $P = 0.006$; parietal lobe: $r = 0.65$, $P = 0.002$; temporal lobe: $r = 0.59$, $P = 0.006$).

In the combined obese and lean group ($n = 26$, 19 obese and seven lean participants), IL-6 and hsCRP were positively associated with BGU ($r = 0.52$, $P = 0.006$, at the cluster level for IL-6 and

$r = 0.52$, $P = 0.007$, at the whole-brain level for hsCRP [Figure S2A, and Figure 2B]). These associations remained significant after controlling for BMI ($P = 0.02$ for both). Insulin-stimulated BGU was positively associated with leptin ($r = 0.48$, $P = 0.01$), but this association was lost after accounting for BMI ($n = 26$). Also, insulin-stimulated BGU was positively associated with the aromatic amino acid, phenylalanine ($r = 0.60$, $P = 0.001$), and the branched-chained amino acid leucine ($r = 0.59$, $P = 0.002$; $n = 26$ [Figure 3]). The correlation between BGU and phenylalanine and leucine, remained significant after adjusting for the M-value ($r = 0.68$, $P = 0.01$, and $r = 0.67$, $P = 0.01$, respectively).

3.2 | After surgery

Six months after surgery, the obese participants had lost 11 BMI units (~24% of their initial body weight), but their BMI remained significantly higher as compared with the controls. The M-value doubled,

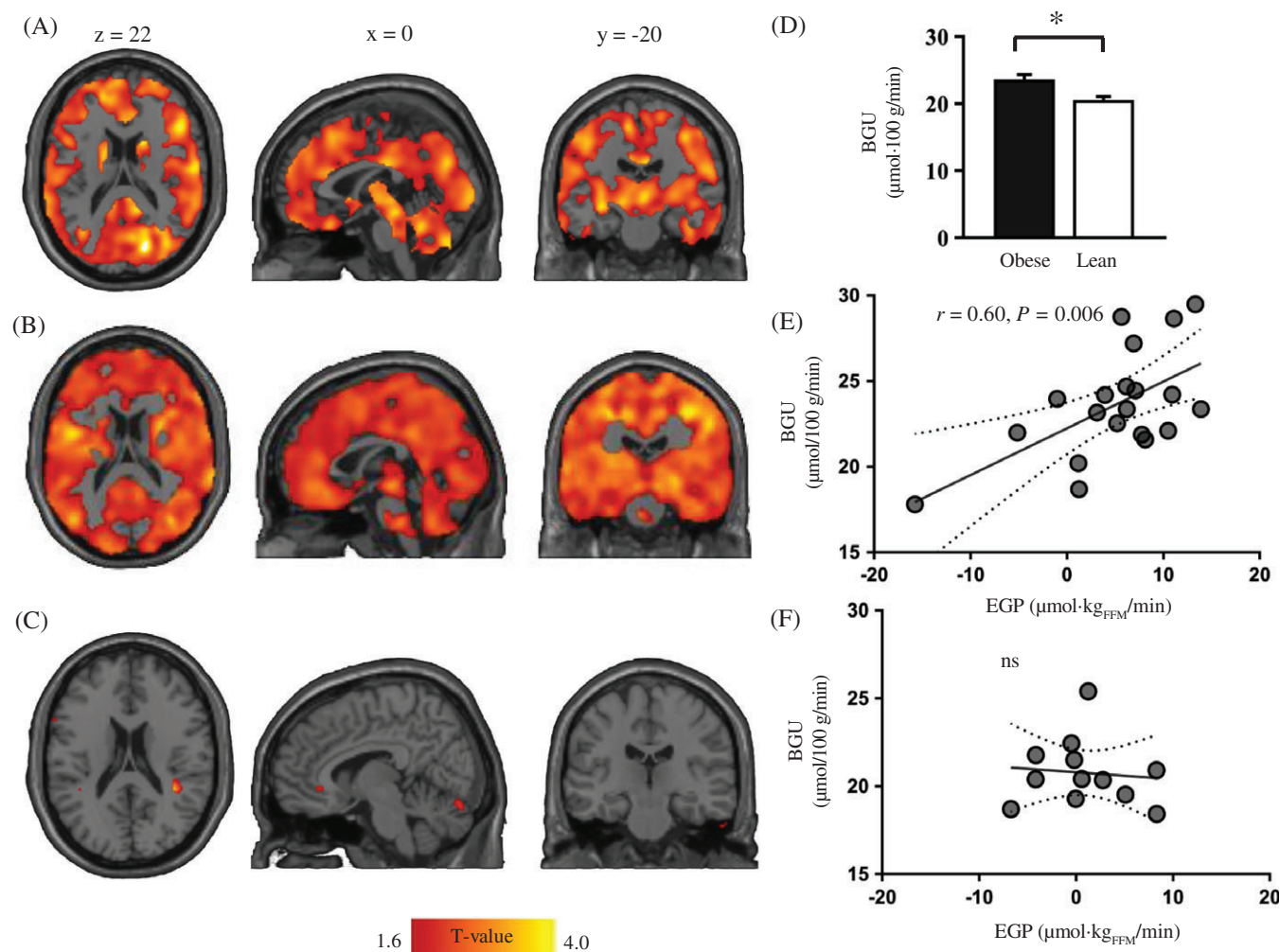


FIGURE 1 A, Statistical parametric mapping (SPM) two-sample *t* test between obese patients preoperatively and controls. Marked brain areas show regions with significantly higher brain glucose uptake (BGU) in the obese patients as compared to controls. Higher *T* values denote larger differences between groups. *P* values <0.05 cluster level, false discovery rate (FDR)-corrected. D, Corresponding boxplots showing the differences in BGU between the two groups. Data are mean ± SEM; **P* < 0.05. B, SPM images of the association between insulin-stimulated BGU and insulin-suppressed endogenous glucose production (EGP) in the obese patients pre-operatively. *P* values <0.05 cluster level, FDR-corrected. C, No association between insulin-stimulated BGU and EGP in lean controls. For images B and C marked brain areas show where the association between BGU and EGP was statistically significant. Higher *T* values denote stronger association between BGU and EGP (coloured bar at the bottom). E, F, Corresponding scatterplots of the association between BGU and EGP in the obese patients and lean participants, respectively

and serum IL-6 and CRP levels decreased significantly. Fasting EGP decreased significantly, in accordance with previous findings.²⁸ Insulin-suppressed EGP showed a small, non-significant decrease and was no longer significantly different from the value in controls (Table 1). BGU was decreased (~5%) but was still higher than in controls (Figure S2B,C) and positively associated with EGP (*r* = 0.56, *P* = 0.02; Figure 2A). Interaction analyses showed no effect of surgical procedure on this association, but the limited sample size does not allow an effect to be conclusively ruled out. The reductions in EGP and BGU were not associated. After surgery, BGU was no longer associated with plasma IL-6 and CRP concentrations.

3.3 | Follow-up

Patients remained weight-stable at 2 and 3 years of follow-up (median [interquartile range] BMI 32.1 [4.1] kg/m² and 32.1 [3.8] kg/m²,

respectively). A higher insulin-stimulated BGU before surgery was associated with a smaller improvement in fasting plasma glucose levels at 2 years (*r* = −0.63, *P* = 0.006 [Figure 2C]). This association persisted after correcting for baseline BMI (*r* = −0.66, *P* = 0.01) or M-value (*r* = −0.72, *P* = 0.02; *n* = 17). In 13 participants who had complete follow-up data for up to 3 years, higher baseline values of insulin-stimulated BGU were still predictive of smaller postoperative decrements of fasting glucose levels (*r* = −0.71, *P* = 0.006; data not shown). By contrast, baseline BGU was unrelated to BMI or HbA1c at follow-up.

4 | DISCUSSION

The main findings of the present study were that insulin-stimulated BGU was positively associated with EGP in morbidly obese but not in

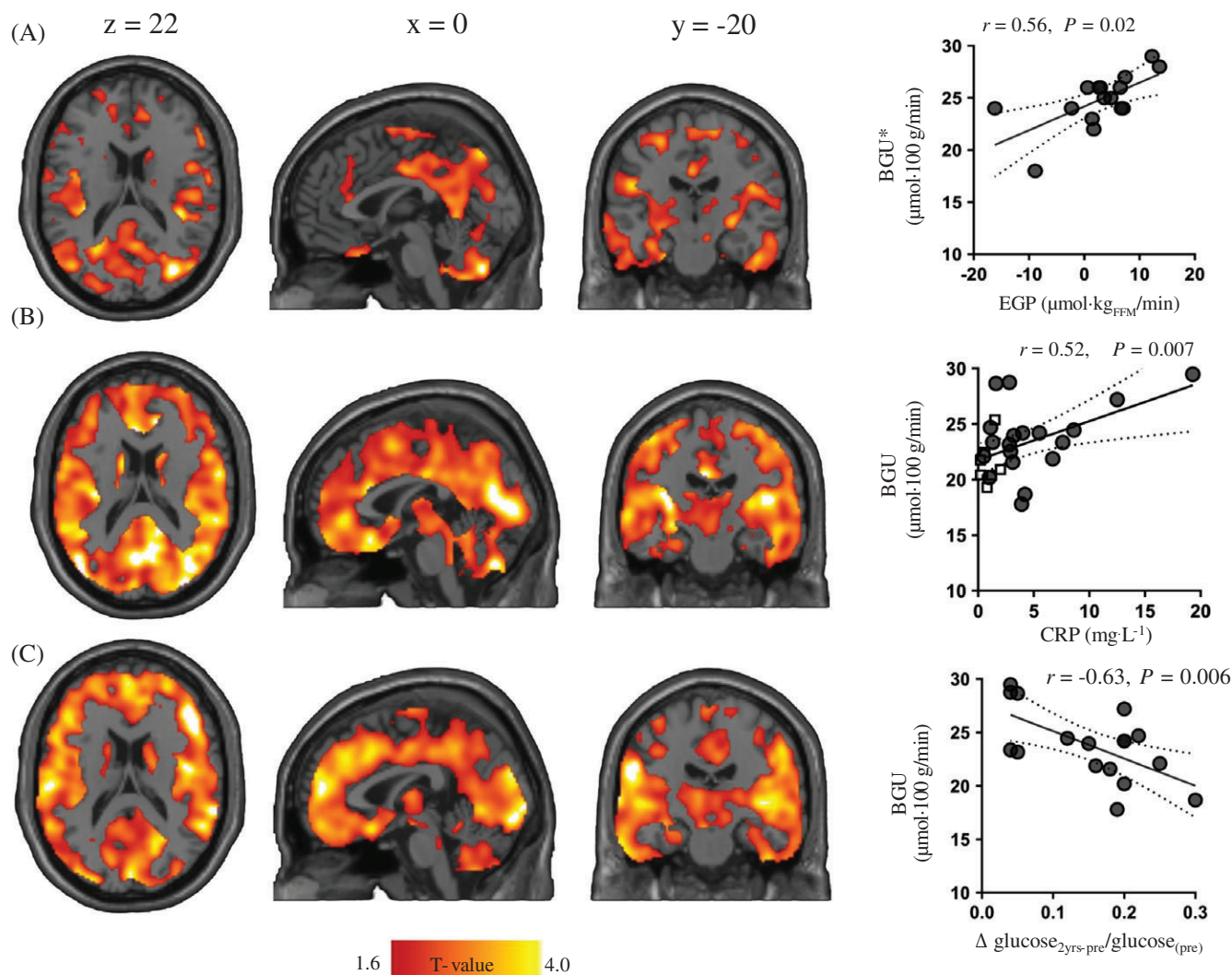


FIGURE 2 A, Statistical parametric mapping (SPM) images of the association between insulin-stimulated brain glucose uptake (BGU) and insulin-suppressed endogenous glucose production (EGP) in the obese patients postoperatively and the corresponding scatterplot. In the scatterplot the mean BGU from the significant voxels only is presented (BGU*). B, SPM images of the association between insulin-stimulated BGU at baseline and plasma C-reactive protein (CRP) and the corresponding scatterplot; grey circles: obese ($n = 19$), white squares: lean controls ($n = 7$). C, SPM images of the association between insulin-stimulated BGU at baseline and change in plasma glucose at 2 years of follow-up in 17 obese patients and the corresponding scatterplot. P values < 0.05 cluster level; FDR-corrected. Higher T values denote stronger associations (coloured bar at the bottom)

lean participants and that this association persisted after significant weight loss resulting from bariatric surgery, with a possible contribution of the preoperative 4-week very-low-energy diet. Moreover, insulin-stimulated BGU predicted metabolic outcome after bariatric surgery. Finally, insulin-stimulated BGU was positively associated with markers of systemic inflammation and with the amino acids phenylalanine and leucine. The brain-EGP axis was explored using ^{18}F -FDG PET, the state-of-the-art methodology for the study of in vivo human metabolism. The plasma ^{18}F -FDG kinetic data were also used to estimate EGP, a method that has been validated against D-[6,6- ^2H]glucose infusion.²³ All analyses regarding BGU data were performed using SPM. This approach is the current community-approved standard in full-volume neuroimaging analysis; it allows voxel-by-voxel analysis of the effects of interest, thereby increasing sensitivity in comparison with ROI analysis. In addition, FDR correction controls the likelihood of false-positive results.

In addition to the present study population,¹³ we have reported in two other study cohorts that insulin resistance was positively associated with insulin-stimulated BGU. We showed that insulin-stimulated BGU was higher in individuals with impaired glucose tolerance than in lean individuals.¹² More recently the same finding was reported in individuals with inherited insulin resistance as compared with age-matched controls.^{12,13,29}

Tschritter et al.³⁰ coined the term “cerebrocortical insulin resistance”, showing using magnetoencephalography that the cerebrocortical insulin effects are blunted both in genetically inherited insulin resistance and in individuals with lifestyle-induced obesity. Heni et al.¹¹ showed that during a euglycaemic hyperinsulinaemic clamp intranasal insulin administration decreases EGP (measured with D-[6,6- ^2H]glucose) in lean but not in overweight individuals. Furthermore, using functional MRI, they found that the hypothalamus and the striatum were involved in this process.¹¹ Our finding of a positive

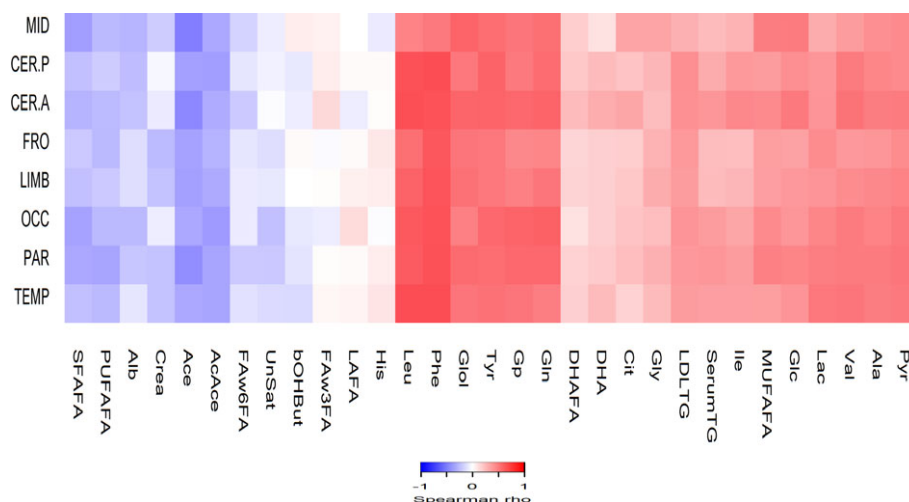


FIGURE 3 Spearman correlations between insulin-stimulated regions of interest of brain glucose uptake (BGU) and fasting metabolites (N = 26). CER-A, anterior cerebellum; CER-P, posterior cerebellum; FRO, frontal lobe; LIMB, limbic lobe; MID, midbrain; OCC, occipital lobe; PAR, parietal lobe; TEMP, temporal lobe. DHA, 22:6, docosahexaenoic acid; DHAF, ratio of 22:6, docosahexaenoic acid to total fatty acids; Faw3, Omega-3 fatty acids; Faw3FA, ratio of Omega-3 fatty acids to total fatty acids; Gic, glucose; Gln, glutamine; Glol, glycerol; Gp, glycoprotein acetylation; HDLC, total cholesterol in HDL; HDL2C, total cholesterol in HDL2; His, histidine; LDLTG, triglycerides in LDL; Leu, leucine; MUFA, monounsaturated fatty acids; MUFAFA, ratio of monounsaturated fatty acids to total fatty acids; Phe, phenylalanine; PUFAFA, ratio of polyunsaturated fatty acids to total fatty acids; Pyr, pyruvate; Serum-TG, serum total triglycerides; SFAFA, ratio of saturated fatty acids to total fatty acids; Tyr, tyrosine; UnSat, estimated degree of unsaturation; VLDLC, total cholesterol in VLDL

association between insulin-stimulated BGU and EGP in morbidly obese participants before and after bariatric surgery may help explain why the addition of intranasal insulin to systemic hyperinsulinaemia failed to suppress EGP in the overweight as compared to the lean participants in that study. Notably, we failed to detect any association between EGP and BGU in the fasting state. Although the reason for the discrepancy in this association between the fasting and insulin-stimulated state needs to be further elucidated, our data are in line with a previous study conducted by Gancheva et al.³¹ who did not observe any effect of intranasal insulin on suppressing EGP during fasting.

It is known that overfeeding rapidly induces insulin resistance.³² Our findings in turn suggest that in morbidly obese individuals the severe calorie restriction and marked weight loss that follow the combination of a 4-week very-low-energy diet period and bariatric surgery are not sufficient to disrupt the association between BGU and EGP. Thus, factors other than high-fat diet and obesity per se might be involved in this interrelation.

One salient finding of the present study was that high insulin-stimulated BGU predicted worse fasting glycaemia 2 to 3 years after surgery; this longitudinal association persisted after adjusting for BMI and whole-body insulin sensitivity. Impaired β -cell glucose sensing and decreased whole-body insulin sensitivity are known independent predictors of worse glycaemic control in individuals without diabetes.³³ In morbidly obese individuals with normal glucose tolerance who undergo bariatric surgery fasting plasma glucose levels fall rapidly after surgery.³⁴ Insulin-stimulated BGU at baseline did not predict worse HbA1c levels or weight gain at 2 or 3 years of follow up, but it was a significant predictor of the metabolic change that is mainly linked with increased EGP, that is, fasting glycaemia; this suggests that the brain-EGP axis may be involved in the deterioration of glucose homeostasis over time. To further test our hypothesis that high

insulin-stimulated BGU is a predictor of worse metabolic outcome we also analysed metabolite data. We found a positive correlation between BGU and known predictors of increased risk of T2D, such as the branched-chain amino acid leucine and the aromatic amino acid phenylalanine.³⁵ These findings are in line with results from the TULIP study, an intervention study with lifestyle modification targeting weight loss. In that study, Tschrirter et al.³⁶ showed that central insulin resistance (assessed by magnetoencephalography) was associated with a smaller decrease in total and visceral adipose tissue and fasting plasma glucose levels and worse adherence to the lifestyle recommendations.

Markers of systemic inflammation were positively associated with insulin-stimulated BGU. Thaler et al.³⁷ have shown that high-fat diet and obesity are associated with neuroinflammation. In a recent study, Zimmer et al.³⁸ showed that brain ¹⁸F-FDG uptake in PET studies is driven by astrocytes. This is in accord with what was originally proposed as the astrocyte-neuron lactate shuttle, whereby astrocytes convert glucose into lactate and supply lactate to neurons,³⁹ but this metabolic paradigm remains controversial.⁴⁰ Altogether, a plausible interpretation of our data could be that the increased BGU in obesity¹³ is, at least in part, attributable to obesity-induced astrocyte proliferation. An obesity-induced astrocyte proliferation could also explain an interplay between brain and EGP.⁴¹ Future PET studies with specific astrocyte ligands are necessary to confirm whether astrocyte proliferation occurs in human obesity.

The present study has some limitations. First, the number of participants was small and, because of the complexity of the study design, we had a relatively large dropout rate. Despite the fact that the postoperative group was smaller, however, the association between BGU and EGP remained significant. Second, it would be interesting to know whether the increased BGU during insulin stimulation affects neuronal functionality, which the present study was not

designed to evaluate. Third, it would be interesting to assess small brain areas, such as the hypothalamus, but the spatial resolution of the PET (6–8 mm) does not allow this.⁴² Finally, the present study documents associations but does not explain the mechanisms underlying the relationship between BGU and EGP.

In summary, insulin-stimulated BGU in obese individuals is increased as compared to lean individuals, and is positively associated with EGP, markers of systemic inflammation, and levels of branched-chain and aromatic amino acids. Additional studies are needed to unravel the peculiar characteristics of brain insulin resistance, and to elucidate whether the increased BGU in insulin resistance might contribute to further deterioration of glucose homeostasis.

ACKNOWLEDGMENTS

The authors thank the staff of the Turku PET Centre for performing the PET imaging. The authors also thank the research nurse Mia Koutu, of Turku PET Centre for data collection.

Conflict of interest

None declared.

Author contributions

E.R., H.I., M.B., M.J.H., J.C.H., L.N., M.S. and P.S. analysed data and literature and drafted the manuscript. H.I., M.S. and J.C.H. conducted the clinical PET studies. M.B. and L.N. analysed the compartmental data analyses. P.I. and P.N. conceived the design. E.F., P.I. and P.N. reviewed the manuscript. All authors approved the final version of the manuscript.

P.N. is the guarantor of this work and, as such, had full access to all the data in the study and takes responsibility for the integrity of the data and the accuracy of the data analysis.


Prior presentation

Parts of this study were presented as an abstract at the 53rd EASD annual meeting at Lisbon.

ORCID

Eleni Rebelos  <http://orcid.org/0000-0003-3050-8692>

Marco Bucci  <http://orcid.org/0000-0002-5206-8651>

Jarna C. Hannukainen  <http://orcid.org/0000-0002-8692-4049>

Miikka-Juhani Honka  <http://orcid.org/0000-0001-9875-5863>

Ele Ferrannini  <http://orcid.org/0000-0002-1384-1584>

Pirjo Nuutila  <http://orcid.org/0000-0001-9597-338X>

REFERENCES

- Kullmann S, Heni M, Hallschmid M, Fritsche A, Preissl H, Häring HU. Brain insulin resistance at the crossroads of metabolic and cognitive disorders in humans. *Physiol Rev*. 2016;96:1169–1209.
- Schwartz MW, Porte D Jr. Diabetes, obesity, and the brain. *Science*. 2005;307:375–379.
- Hopkins DF, Williams G. Insulin receptors are widely distributed in human brain and bind human and porcine insulin with equal affinity. *Diabet Med*. 1997;14:1044–1050.
- Taylor SI. Deconstructing type 2 diabetes. *Cell*. 1999;97:9–12.
- Shimazu T, Fukuda A, Ban T. Reciprocal influences of the ventromedial and lateral hypothalamic nuclei on blood glucose level and liver glycogen content. *Nature*. 1966;210:1178–1179.
- Obici S, Zhang BB, Karkanias G, Rossetti L. Hypothalamic insulin signaling is required for inhibition of glucose production. *Nat Med*. 2002;8:1376–1382.
- Inoue H, Ogawa W, Asakawa A, et al. Role of hepatic STAT3 in brain-insulin action on hepatic glucose production. *Cell Metab*. 2006;3:267–275.
- Marty N, Dallaporta M, Thorens B. Brain glucose sensing, counterregulation, and energy homeostasis. *Physiology (Bethesda)*. 2007;22:241–251.
- Ramnanan CJ, Saraswathi V, Smith MS, et al. Brain insulin action augments hepatic glycogen synthesis without suppressing glucose production or gluconeogenesis in dogs. *J Clin Invest*. 2011;121:3713–3723.
- Dash S, Xiao C, Morgantini C, Koulajian K, Lewis GF. Intranasal insulin suppresses endogenous glucose production in humans compared with placebo in the presence of similar venous insulin concentrations. *Diabetes*. 2015;64:766–774.
- Heni M, Wagner R, Kullmann S, et al. Hypothalamic and striatal insulin action suppresses endogenous glucose production and may stimulate glucose uptake during hyperinsulinemia in lean but not in overweight men. *Diabetes*. 2017;66:1797–1806.
- Hirvonen J, Virtanen KA, Nummenmaa L, et al. Effects of insulin on brain glucose metabolism in impaired glucose tolerance. *Diabetes*. 2011;60:443–447.
- Tuulari JJ, Karlsson HK, Hirvonen J, et al. Weight loss after bariatric surgery reverses insulin-induced increases in brain glucose metabolism of the morbidly obese. *Diabetes*. 2013;62:2747–2751.
- Conte C, Fabbrini E, Kars M, Mittendorfer B, Patterson BW, Klein S. Multiorgan insulin sensitivity in lean and obese subjects. *Diabetes Care*. 2012;35:1316–1321.
- Immonen H, Hannukainen JC, Iozzo P, et al. Effect of bariatric surgery on liver glucose metabolism in morbidly obese diabetic and non-diabetic patients. *J Hepatol*. 2014;60:377–383.
- Helmio M, Victorzon M, Ovaska J, et al. SLEEVEPASS: a randomized prospective multicenter study comparing laparoscopic sleeve gastrectomy and gastric bypass in the treatment of morbid obesity: preliminary results. *Surg Endosc*. 2012;26:2521–2526.
- Makinen J, Hannukainen JC, Karmi A, et al. Obesity-associated intestinal insulin resistance is ameliorated after bariatric surgery. *Diabetologia*. 2015;58:1055–1062.
- DeFronzo RA, Tobin JD, Andres R. Glucose clamp technique: a method for quantifying insulin secretion and resistance. *Am J Physiol*. 1979;237:E214–E223.
- Hamacher K, Coenen HH, Stocklin G. Efficient stereospecific synthesis of no-carrier-added 2-[¹⁸F]-fluoro-2-deoxy-D-glucose using aminopolyether supported nucleophilic substitution. *J Nucl Med*. 1986;27:235–238.
- Alenius S, Ruotsalainen U. Bayesian image reconstruction for emission tomography based on median root prior. *Eur J Nucl Med*. 1997;24:258–265.
- Wu HM, Bergsneider M, Glenn TC, et al. Measurement of the global lumped constant for 2-deoxy-2-[¹⁸F]fluoro-D-glucose in normal human brain using [¹⁵O]water and 2-deoxy-2-[¹⁸F]fluoro-D-glucose positron emission tomography imaging. A method with validation based on multiple methodologies. *Mol Imaging Biol*. 2003;5:32–41.
- The International Commission on Radiological Protection. *Report of the Task Group on Reference Man. A Report Prepared by a Task Group of Committee 2 of the International Commission on Radiological Protection*. Oxford, UK: Pergamon Press; 1975.
- Iozzo P, Gastaldelli A, Jarvisalo MJ, et al. 18F-FDG assessment of glucose disposal and production rates during fasting and insulin stimulation: a validation study. *J Nucl Med*. 2006;47:1016–1022.
- Camastra S, Manco M, Mari A, et al. Beta-cell function in morbidly obese subjects during free living: long-term effects of weight loss. *Diabetes*. 2005;54:2382–2389.

25. RC Team. *R: A Language and Environment for Statistical Computing*. Vienna, Austria: R Foundation for Statistical Computing; 2014.
26. Warnes GR, Bolker B, Bonebakker L, et al. *Gplots: Various R Programming Tools for Plotting Data*. R Package Version 3.0.1. CRAN; 2016.
27. Benjamini Y, Hochberg Y. Controlling the false discovery rate - a practical and powerful approach to multiple testing. *J R Stat Soc Ser B Stat Methodol*. 1995;57:289-300.
28. Camastra S, Gastaldelli A, Mari A, et al. Early and longer term effects of gastric bypass surgery on tissue-specific insulin sensitivity and beta cell function in morbidly obese patients with and without type 2 diabetes. *Diabetologia*. 2011;54:2093-2102.
29. Latva-Rasku A, Honka MJ, Stancakova A, et al. A partial loss-of-function variant in AKT2 is associated with reduced insulin-mediated glucose uptake in multiple insulin sensitive tissues: a genotype-based callback positron emission tomography study. *Diabetes*. 2018;67:334-342.
30. Tschritter O, Preissl H, Hennige AM, et al. The cerebrocortical response to hyperinsulinemia is reduced in overweight humans: a magnetoencephalographic study. *Proc Natl Acad Sci U S A*. 2006;103:12103-12108.
31. Gancheva S, Koliaki C, Bierwagen A, et al. Effects of intranasal insulin on hepatic fat accumulation and energy metabolism in humans. *Diabetes*. 2015;64:1966-1975.
32. Wang J, Obici S, Morgan K, Barzilai N, Feng Z, Rossetti L. Overfeeding rapidly induces leptin and insulin resistance. *Diabetes*. 2001;50:2786-2791.
33. Walker M, Mari A, Jayapaul MK, Bennett SMA, Ferrannini E. Impaired beta cell glucose sensitivity and whole-body insulin sensitivity as predictors of hyperglycaemia in non-diabetic subjects. *Diabetologia*. 2005;48:2470-2476.
34. Jorgensen NB, Jacobsen SH, Dirksen C, et al. Acute and long-term effects of Roux-en-Y gastric bypass on glucose metabolism in subjects with Type 2 diabetes and normal glucose tolerance. *Am J Physiol Endocrinol Metab*. 2012;303:E122-E131.
35. Guasch-Ferré M, Hruby A, Toledo E, et al. Metabolomics in prediabetes and diabetes: a systematic review and meta-analysis. *Diabetes Care*. 2016;39:833-846.
36. Tschritter O, Preissl H, Hennige AM, et al. High cerebral insulin sensitivity is associated with loss of body fat during lifestyle intervention. *Diabetologia*. 2012;55:175-182.
37. Thaler JP, Yi CX, Schur EA, et al. Obesity is associated with hypothalamic injury in rodents and humans. *J Clin Invest*. 2012;122:153-162.
38. Zimmer ER, Parent MJ, Souza DG, et al. [18F]FDG PET signal is driven by astroglial glutamate transport. *Nat Neurosci*. 2017;20:393-395.
39. Pellerin L, Magistretti PJ. Glutamate uptake into astrocytes stimulates aerobic glycolysis: a mechanism coupling neuronal activity to glucose utilization. *Proc Natl Acad Sci U S A*. 1994;91:10625-10629.
40. Diaz-Garcia CM, Mongeon R, Lahmann C, et al. Neuronal stimulation triggers neuronal glycolysis and not lactate uptake. *Cell Metab*. 2017;26:361-374.e364.
41. Parsons MP, Hirasawa M. ATP-sensitive potassium channel-mediated lactate effect on orexin neurons: implications for brain energetics during arousal. *J Neurosci*. 2010;30:8061-8070.
42. Teräs M. Performance and methodological aspects in positron emission tomography. Turku, Turun Yliopisto 2008.

SUPPORTING INFORMATION

Additional supporting information may be found online in the Supporting Information section at the end of the article.

How to cite this article: Rebelos E, Immonen H, Bucci M, et al. Brain glucose uptake is associated with endogenous glucose production in obese patients before and after bariatric surgery and predicts metabolic outcome at follow-up. *Diabetes Obes Metab*. 2018;1-9. <https://doi.org/10.1111/dom.13501>